# Charge ordering and onedimensional magnetism in $Yb_4As_3$

Burkhard SCHMIDT, Hidekazu AOKI, Tomasz CICHOREK, Philipp GEGENWART, Akira OCHIAI[1] and Frank STEGLICH

*Max Planck Institute for the Chemical Physics of Solids, Nöthnitzer Str. 40, 01187 Dresden, Germany*
[1] *Center for Low Temperature Science, Tohoku University, Sendai 980-8578, Japan*

We discuss a mechanism leading to heavy-fermion behavior and quasi-onedimensional magnetism based on the charge-ordering transition out of a threedimensional homogeneous mixed-valence state. We focus the discussion on the realization of this scenario in $Yb_4As_3$ and the P- and Sb-substituted mixed compounds. We present recent experimental results on the low-temperature magnetic susceptibility and specific heat in an applied magnetic field. At temperatures below 1 K, we have observed spin glass behavior due to a small interchain coupling and disorder.

KEYWORDS: $Yb_4As_3$, charge ordering, onedimensional Heisenberg antiferromagnet, heavy fermion, spin glass

## §1. Introduction

Onedimensional spin systems show a large variety of quantum many-body effects, which are particularly interesting because of the lack of classical analogs in most cases. In the last few years, a new route to onedimensional spin physics has been found in compounds that exhibit a charge-ordering transition. In such compounds no localized spins on fixed atomic positions exist at high temperatures. They rather are homogeneous mixed-valence (semi-)metals or valence-fluctuating insulators at high temperatures. Their $3d$ or $4f$ electrons are strongly correlated and close to localization, i. e., having a low effective kinetic energy. If the intersite Coulomb repulsion in such compounds is large enough it may dominate the kinetic energy and, once the charge-disorder entropy due to hopping is low enough, lead to a charge-ordering transition at a critical temperature $T_{\rm co}$ below which the valence fluctuations are suppressed. The resulting inhomogeneous mixed-valence state consists of two species of ions with valence $Z$ and $Z+1$. This transition may be compared to a Wigner crystallization on a lattice,[1)] and its earliest example is the Verwey transition in magnetite,[2)] although this picture turned out to be too simplified for this compound.

If one of the valence species, say $Z$, has no magnetic moment, the charge ordering transition may lead to a structure where the species $Z+1$ with spin $S$ occupies only sites which lie on well isolated chains (not necessarily linear) with only weak exchange interactions between the chains, thus creating a quasi-onedimensional system of localized atomic spins at low temperatures out of the high-temperature state. This scenario has been found to be realized in the $3d$-layer compound sodium vanadate[3)] where in addition an exchange dimerization in the chains leads to a spin-gap formation. The best studied and well confirmed system for the charge-ordering route to onedimensional spin physics is the $4f$-pnictide compound $Yb_4As_3$. In this article, we discuss both the experimental and theoretical work done on this material, focussing on the properties of the charge-ordering transition and its low-temperature magnetic characteristics.

This article is organized as follows: In the next section, we will summarize in short the charge-ordering transition in terms of a mean-field model for the intersite Coulomb interaction and the crossover to an effective onedimensional spin system at temperatures far below $T_{\rm co}$. Section 3 contains a discussion of the response of $S=1/2$ spin chains in $Yb_4As_3$ to external magnetic fields. In section 4, we present new results for the spin-glass freezing found at very low temperatures where the interchain coupling and disorder effects become important. Finally, the last section gives our conclusion and outlook.

## §2. Charge-ordering transition

The high-temperature phase of $Yb_4As_3$ is cubic (lattice constant $a = 8.788$ Å) and has the anti-$Th_3P_4$ crystal structure with space group $I\bar{4}3d$. The Yb-ions occupy the Phosphorus sites on the threefold symmetry axes, the As-ions are located on the Thorium sites. The arrangement of the Yb-sites can be viewed as being aligned on four families of interpenetrating chains oriented parallel to the space diagonals of a cube, known as body-centered cubic rod packing.[4)]

Chemical-valence counting assuming that the As-ions are trivalent shows that three quarter of the Yb-ions have filled $4f$ shells with a valency 2+, and one quarter with valency 3+ has one hole in the $f$-shell ($f^{13}$-configuration). In the high-temperature phase, all Yb-sites are equivalent, and the holes in the $f$-shells are moving between the Yb-ions due to hybridization with the As-$4p$ holes: The compound is in a metallic intermediate-valence state with an average valency of 2.25+. Mössbauer-spectroscopy data on $^{170}$Yb show that below 50 K the system contains about $20 \pm 5\,\%$ $Yb^{3+}$-ions characterized by a $4f^{13}$-configuration and a $J=7/2$ ground-state multiplet.[5)]

At $T_{\rm co} \simeq 295$ K, a first-order structural phase transition has been observed which is accompanied by discontinuities of various quantities, e. g., the electrical resistivity

and the Hall coefficient.[6] At the structural transition, $Yb_4As_3$ shrinks along one of the four equivalent chain directions, in the following called the "short" chain.[7] The four formerly equivalent chains are subdivided into one along the $\langle 111 \rangle$-direction and the three remaining "long" chains. This transition is approximately volume-conserving. The resulting trigonal unit cell has space group R3c with the short chain being parallel to the main axis. The trigonal angle is 90.8 degrees.[6,7]

Along with the transition to the trigonal phase, a charge ordering of the Yb-ions occurs: The $4f$ electronic state of $Yb_4As_3$ changes from a valence-fluctuating state in the cubic phase to a slightly incomplete charge-ordered state which can be expressed as $Yb^{3+}Yb_3^{2+}As_3^{3-}$, where the $Yb^{3+}$-ions are arranged predominantly on the short chain parallel to, e.g., the former cubic $\langle 111 \rangle$ direction. The low-temperature Hall coefficient $R_H$ is positive, implying dominant hole conduction. Assuming the presence of only one type of charge carriers, their density is as small as approximately 0.001 per $Yb^{3+}$-ion.

The model to explain the transition is based on a band Jahn-Teller effect of correlated electrons (CBJT):[8] The fifty-six Yb $4f$-bands have an overall width of $\sim 0.2\,\mathrm{eV}$ which arises from effective $f$–$f$ hopping via hybridization with pnictide valence states.[9] To reduce the complexity of the $f$-bands the assumption is made that they can be described by four degenerate quasi-onedimensional bands associated with the chains. The filling of each of these bands corresponds to the number of Yb-$4f^{13}$ states in the chain associated with it. Since the $Yb^{3+}$-ions have a smaller radius than the $Yb^{2+}$-ions, it is natural to think of the CBJT transition as being related to the ordering of $Yb^{3+}$-ions along the space diagonal $\langle 111 \rangle$. Moreover, in this description, charge ordering on chains and the band Jahn-Teller effect are completely equivalent.

Such a model is rather similar to the Labbé-Friedel model for $3d$ states in A 15 compounds[10] where chains parallel to the cubic axes are the dominant structural elements. Although such models may not be literally true due to the three-dimensionality of the electronic states, they describe the important aspect that a strain-coupling to the degenerate band states may easily lead to distortions of the cubic structure and simultaneous repopulation among the $4f$ states of $Yb_4As_3$.

There is a strong deformation-potential coupling typical for intermediate-valence systems which removes this degeneracy by a trigonal CBJT-distortion. This deformation potential describes the effect of the nearest-neighbor Coulomb repulsion between the Yb-sites. (Note that the three nearest Yb-neighbors of an Yb-ion on one chain are located on chains belonging to the other three families.)

The particular ordering of the $Yb^{3+}$-ions described here was confirmed clearly by perturbed angular-correlation (PAC) measurements,[11] and a direct proof for the charge ordering in $Yb_4As_3$ was given by polarized-neutron scattering.[12,13] The stabilization of the $Yb^{3+}$ states on the short chains was further supported by temperature dependent spectral changes in high-resolution photoemission spectroscopy.[14] A recent resonant X-ray diffraction experiment on the Yb $L_3$-absorption edge gave an additional direct evidence for the particular onedimensional charge order described here.[15]

An estimation of the Madelung energy gain of the $4f$-holes for several different charge-ordered states done by performing the Ewald summations showed that the ordering of the $Yb^{3+}$-ions along one single space diagonal does *not* correspond to the configuration minimizing the static Coulomb energy.[16,17] Instead, an equal but static distribution of the $Yb^{3+}$-ions on all four cubic space diagonals maximizes the distance between any two neighboring $4f^{13}$ states, thereby minimizing their mutual Coulomb repulsion, leading to a lower total energy.

The Yb sites in this hypothetical $P2_13$ crystal structure would have four nonequivalent Wyckoff positions 4a,.3., with $x_1 \ldots x_4$ along the space diagonals, and their Madelung energy is 6 mRyd per formula unit lower than that of the trigonal R3c structure realized.[17] However, an LSDA total-energy calculation yields a trigonal ground state with an energy by 2 mRyd per f. u. lower than that of the cubic phase, for the following reason:[17] Leaving out the pnictide positions, each Yb-ion on one particular chain has three nearest-neighbor Yb ions belonging to the three other chain families; its two next-nearest neighbors are located on the same chain. Therefore, in the trigonal structure, each $Yb^{2+}$-ion has one $Yb^{3+}$- and two $Yb^{2+}$-ion in its nearest-neighbor shell, and all $Yb^{2+}$-sites are symmetry equivalent. In the cubic charge-ordered phase, viewed along one arbitrary space diagonal, three $Yb^{2+}$-ions are followed by an $Yb^{3+}$-ion, and this pattern is repeated in each diagonal-chain direction. The middle of any three $Yb^{2+}$-ions has three $Yb^{3+}$-ions as nearest neighbors, while the two others have only $Yb^{2+}$-ions as nearest neighbors, leading to a slight charge disproportionation. This charge difference of 0.05 electron charges costs 8 mRyd per f. u., to be added to the total energy.

The description of the structural transition in terms of the CBJT model does not yet contain the strong intra-ionic Coulomb forces between the holes at the Yb-sites. Therefore, it is applicable only above $T_{co}$, where the number of holes per Yb-site is 1/4 and somewhat below $T_{co}$. At low temperatures, where the filling of the effective band associated with the "short" chain approaches 1, the Coulomb interactions and the strong correlations which they imply become crucial: For vanishing magnetic field and at temperatures below about 10 K, the thermodynamic properties of $Yb_4As_3$ resemble that of a typical heavy-fermion metal. Above $T \approx 0.5\,\mathrm{K}$, the specific heat is dominated by a term linear in temperature, $C = \gamma T$, with $\gamma \approx 200\,\mathrm{mJ/(K^2 \cdot mol)}$.[18] Upon lowering the temperature, $C(T)/T$ shows a steep increase with a low-temperature asymptotic $T^{-3}$ dependence and a shoulder-like anomaly near $T = 0.2\,\mathrm{K}$. We shall return to these low-$T$ results in sections 3 and 4. The static magnetic susceptibility is almost $T$-independent between 10 K and 2 K and extrapolates for $T \to 0$ to a rather large value of $\chi(T \to 0) \approx 3 \cdot 10^{-2}\,\mathrm{emu/mol}$. The Sommerfeld-Wilson ratio $R = \pi^2 k_B^2 \chi(T \to 0)/(3\mu_{\mathrm{eff}}^2 \gamma)$ is of the order of unity. For very low temperatures, however, $\chi(T)$ like $C(T)/T$ shows a strong increase with decreasing temperature.

In contrast to metals with an enhanced density of

states for low-energy fermionic charge degrees of freedom, $Yb_4As_3$ has almost no charge carriers, implying that the standard Kondo picture for the origin of these excitations cannot be applied. Instead, as the short chain approaches half-filling, the strong on-site Coulomb interaction in this chain leads to an effective Heisenberg-type of interaction with a magnetic exchange energy $J$ responsible, e. g., for the very large specific heat for temperatures with $k_BT/J \ll 1$. The magnetic excitations correspond to those of an antiferromagnetic quasi-onedimensional "$S = 1/2$" Heisenberg chain, where $\mathbf{S}$ is the pseudospin describing the lowest Kramers doublet of $Yb^{3+}$, slightly modified by the presence of about 0.001 holes per $Yb^{3+}$-ion.

Thermal and transport measurements on P- and Sb-doped samples gave further experimental evidence for the scenario described here:[19–21] With increasing concentration $x$ of Phosphorus, the electrical resistivity of $Yb_4(As_{1-x}P_x)_3$ grows drastically, and with $x = 0.3$ it is nearly insulating, while the specific heat and the magnetic susceptibility are almost the same as those of pure $Yb_4As_3$. With increasing Sb content $x$, the absolute value of the resistivity of $Yb_4(As_{1-x}Sb_x)_3$ decreases due to the increase of the number of charge carriers and the system becomes more metallic while again the specific-heat $\gamma$ value is roughly the same as in the pure compound and thus almost independent of the carrier concentration. However, at 29 % Sb-doping, the charge ordering seems to disappear, i. e., no discontinuity in thermodynamic and transport properties could be observed.

The crossover to the low-$T$ spin-chain structure was well confirmed by inelastic-neutron scattering experiments by Kohgi et al.[12,22] They show that the low-temperature magnetic excitations in $Yb_4As_3$ are indeed very well described by the onedimensional spin-excitation spectrum $\omega(q) = (\pi/2)\sin(aq)$ as described by des Cloizeaux and Pearson[23] where $q$ is the wave number in ⟨111⟩-direction and $a$ the distance between the $Yb^{3+}$-ions along the short chains. More precisely, this dispersion describes the lower boundary of the two-spinon continuum, i. e., a continuum of spin excitations whose spectral function for a fixed momentum $q$ diverges at this lower boundary.[24,25] From the maximum observed spin excitation energy of 3.8 meV $\approx k_B \cdot 40$ K at $q = \pi/(2a)$ one obtains $J \approx k_B \cdot 25$ K in good agreement with the energy scale $k_BT^*$ estimated from the value of the specific-heat coefficient as measured.

## §3. Field-induced spin gap

For an antiferromagnetic $S = 1/2$ Heisenberg chain with exchange energy $J$, one would expect a magnetic-field dependence of the thermodynamic observables to be of the order $(\mu_{\text{eff}}B/J)^2$, i. e., about one percent at a few Tesla uniformly for all temperatures with $k_BT/J \ll 1$. In contrast, the behavior of the specific heat is quite different:

At temperatures below 2 K, upon increasing the applied magnetic field, $\gamma = C(T)/T$ becomes drastically reduced slightly above the temperature at which the low-$T$ upturn sets in, while at somewhat higher temperatures a broad hump forms which is continuously shifted towards

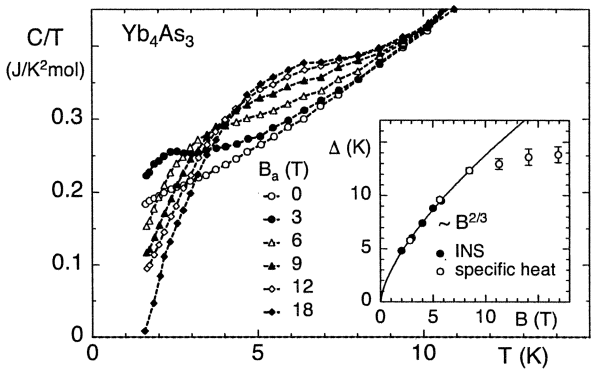


Fig. 1. Specific heat of a polydomain $Yb_4As_3$-sample at varying magnetic fields $B_a$, applied along the cubic ⟨111⟩ direction. The inset shows the spin-excitation gap $\Delta$ as derived from inelastic-neutron scattering (INS)[34] and the specific-heat analysis discussed in the text. The solid line represents the relation $\Delta(B) = 2.97\,\text{K}\,(B/\text{T})^{2/3}$.

higher temperatures. Already at a field $B = 4$ T, $\gamma(B)$ is strongly suppressed, indicating the opening of a gap in the low-energy excitation spectrum.

A detailed analysis of the corresponding anomalies found in thermal-expansion experiments performed on samples with varying domain configurations showed that the occurrence and the quantitative behavior of this field dependence requires a finite magnetic-field component perpendicular to the short (i. e., the $S = 1/2$) chains.[26,27] Several mechanisms have been proposed to account for the observations: (a) a small interchain coupling $J'$ between adjacent parallel short chains,[28] (b) an intrachain dipole–dipole interaction,[29] (c) solitary solutions of the classical sine-Gordon model of a onedimensional Heisenberg antiferromagnet with a weak uniaxial anisotropy plus a weak interchain coupling.[26] For the latter, the magnetic-field dependence of the soliton rest energy $E_S$ is expected to be $E_S \propto B^\nu$ with an exponent $\nu = 1$. In contrast, the exponent deduced from fits to the specific-heat, thermal-expansion and thermal-conductivity data has a value of $\nu \approx 2/3$.[27]

A fourth possible scenario for the field-induced excitation gap in $Yb_4As_3$[30,31] has been modeled similar to the mechanism which was used successfully to explain the behavior of the quasi-onedimensional system Cu benzoate in a magnetic field:[32] An induced staggered magnetic field was proposed as the driving force for the gap opening in this case,[33] whereby both an alternating $g$-tensor and the Dzyaloshinskii-Moriya (DM) interaction may account for this staggered field. In the case of $Yb_4As_3$, the local $C_3$ symmetry at the Yb-sites on the short chains, and the absence of a center of inversion symmetry between two adjacent $Yb^{3+}$-ions allow for a uniaxial anisotropy in the symmetric part of the spin exchange as well as for the presence of an additional antisymmetric DM spin exchange interaction. The glide reflection with the glide vector parallel to the $Yb^{3+}$-chains requires an alternating sign for this antisymmetric part, if present. The same symmetry constraints apply to the $g$-tensor.

An investigation of the wavefunctions of the $J = 7/2$ ground-state multiplet uncovered an additional hidden

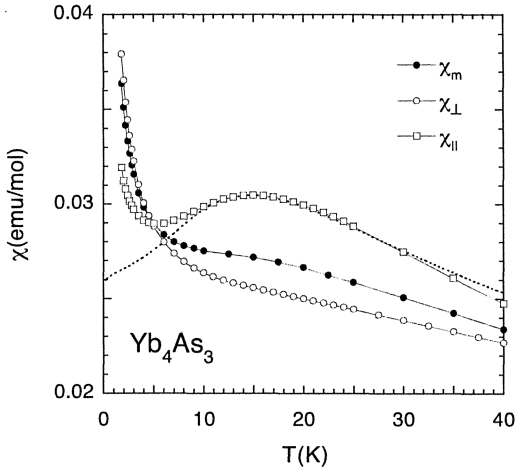


Fig. 2. Temperature dependence of the susceptibility of $Yb_4As_3$ along ($\chi_\parallel$) and perpendicular ($\chi_\perp$) to the trigonal axis as well as that of a polydomain sample ($\chi_m$).[38] The dotted line shows a fit to the $\chi_\parallel$ data including the uniform susceptibility of the $S = 1/2$ antiferromagnetic Heisenberg chain $\chi_{1D}$[39] with exchange coupling $J = 26\,K$[40] and a constant van Vleck term $\chi_{vV}$.

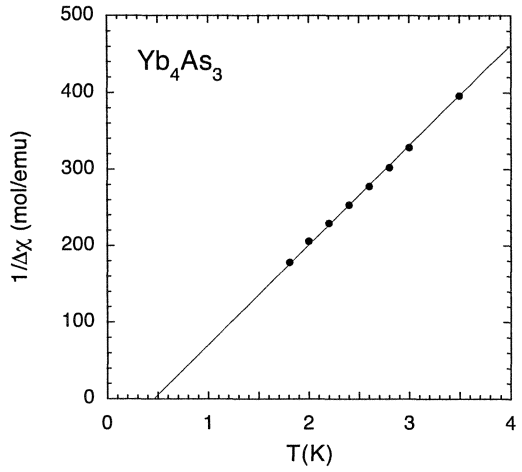


Fig. 3. Inverse of the static magnetic susceptibility $\Delta\chi_\parallel = \chi_\parallel - (\chi_{1D} + \chi_{vV})$ (see dotted line in Figure 2) vs. $T$.[37]

isotropy of the effective Hamiltonian:[31] At *zero field*, this Hamiltonian is equivalent to the onedimensional *isotropic* $S = 1/2$ Heisenberg antiferromagnet. For a *finite* applied magnetic field $\mathbf{B}$, the field component perpendicular to the short chains induces a staggered field of the form $\mathbf{b} \propto g_\perp \cdot \mathbf{n} \times \mathbf{B}$, where $\mathbf{n}$ is a unit vector pointing in the chain direction.

Using the quantum sine Gordon (SG) model as a low-energy effective field theory of the Heisenberg model,[30,33] the staggered field induces an excitation gap $\Delta \propto J^{1/3} b^{2/3}$ in very good agreement with our experimental observations at low applied magnetic fields. However, the quantum SG model is a continuum approximation valid only for fields with $h = g_\perp \mu_B B/J \ll 1$. For a higher field strength, deviations from the $b^{2/3}$-dependence occur, as will be discussed below.

Recent inelastic-neutron scattering experiments using magnetic fields up to 5.8 T showed that the excitation spectrum changes drastically from the two-spinon continuum at zero field to a sharp one at finite fields with a finite excitation energy, providing a direct proof for the opening of the spin gap.[34,35] The derived magnetic-field dependence of this gap follows $\Delta(B) \propto B^{2/3}$.

We have performed additional specific-heat measurements in high magnetic fields of up to 18 T to further study the field-dependence of the excitation gap, see Figure 1. The experiments were done on a polydomain sample with the magnetic field oriented parallel to one cubic space diagonal of it. Therefore about 75 % of the short chains formed due to the charge ordering had a finite field component perpendicular to their orientation with an effective value $B = B_a \cdot \sin(70°)$, where $B_a$ denotes the strength of the externally applied magnetic field.

After subtracting the phonon contribution determined from the zero-field data, we have determined the positions of the resulting broad maxima in the temperature dependence of the $C(T,B)/T$-curves. According to recent finite-temperature density-matrix renormalization group (DMRG) calculations, these maxima are located at about $0.4 \cdot \Delta/k_B$.[36] Using this relation, we have extracted $\Delta(B)$ from our specific-heat data. $\Delta(B)$ follows the predicted $B^{2/3}$ dependence for $B \leq 9\,T$.

Upon increasing $B$ further, the Zeeman energy becomes comparable to the intrachain coupling. This leads to the destruction of the onedimensional antiferromagnetic state, and a crossover to a ferromagnetic polarization of the spins occurs, accompanied by a flattening of the $\Delta(B)$- dependence. According to Uimin et al., the excitation gap even disappears at a transverse field $h = g_\perp \mu_B B/J \approx 2$, at which a full ferromagnetic alignment of the spins is reached.[29] Our experiments show that indeed the magnetic-field dependence of $\Delta$ saturates for fields above 14 T. For $g_\perp = 1.2$ as determined by polarized-neutron diffraction,[35] this saturation field corresponds to $h = 0.42$.

## §4. Spin-glass freezing

For an investigation of the anisotropies in various thermodynamic quantities, a small uniaxial pressure parallel to one of the ⟨111⟩ directions must be applied in the cubic phase prior to cooling down through $T_{co}$ in order to avoid a formation of domains in the trigonal phase at low temperatures.

The anisotropy of the magnetic susceptibility of a monodomain $Yb_4As_3$ crystal, see Figure 2, was first measured by Aoki et al. from room temperature down to 2 K in a SQUID magnetometer.[37,38] In this measurement, the monodomain formation was almost perfect since (a) with increasing uniaxial pressure a saturation of the pressure-induced anisotropy $\chi_\parallel(15\,K)/\chi_\perp(15\,K)$ was observed ($\chi_\parallel$, $\chi_\perp$ denote the susceptibility along and perpendicular to the trigonal axis) and (b) the average susceptibility $\bar{\chi} = \chi_\parallel/3 + 2\chi_\perp/3$ coincided with that of the polydomain state ($\chi_m$), studied without uniaxial pressure.

Above 7 K the $T$-dependence of $\chi_\parallel$ is well described by the sum of a constant van Vleck contribution and the uniform susceptibility of the $S = 1/2$ antiferromagnetic Heisenberg chain[39] assuming an intrachain exchange coupling $J = 26\,K$.[40] On the other hand, the huge upturn of $\chi_\perp$ would be in accordance with the prediction

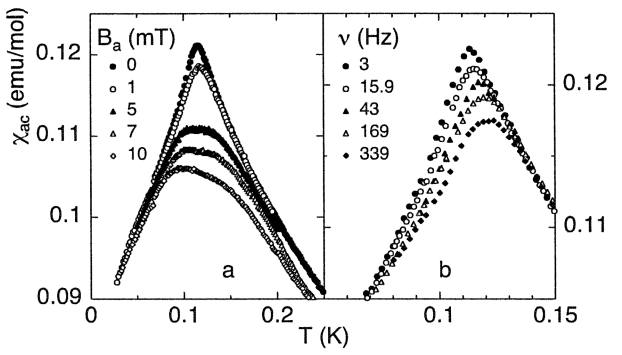


Fig. 4. Temperature dependence of the ac-susceptibility with $B_{ac} = 0.1\,\mathrm{mT}$ in different static fields $B_a$ applied along the cubic ⟨111⟩ direction of polydomain $Yb_4As_3$ (a), and measured at different frequencies $\nu$ in $B_a = 0$ (b).

of the staggered-field model which causes a $1/T$ divergence of the susceptibility.[30] However, since no staggered field is induced for magnetic fields applied *parallel* to the trigonal axis, i. e., *parallel* to the spin chains, the upturn of $\chi_{\|}(T)$ below 7 K cannot be explained within the staggered-field SG model.

The inverse of this deviation $\Delta\chi_{\|} = \chi_{\|} - (\chi_{1D} + \chi_{vv})$ as a function of temperature follows a Curie-Weiss law $\Delta\chi_{\|} = C/(T - \Theta)$ with a positive Weiss temperature $\Theta$, indicating a dominating ferromagnetic interaction,[37] see Figure 3. This is not related to possible magnetic impurities: The upturn does not significantly increase with decreasing sample quality.[37] Since the charge ordering in $Yb_4As_3$ is not perfect one might relate $\Delta\chi_{\|}$ to a contribution of the "free spins" at the chain edges. By doping with $Lu^{3+}$-ions on the $Yb^{3+}$-sites in $(Yb_{1-x}Lu_x)_4As_3$, one can increase the number of edges of the onedimensional chains. This leads to an additional Curie-Weiss contribution in the low-temperature susceptibility which is proportional to $x$.[37] This contribution, however, shows a negative Weiss temperature indicating an antiferromagnetic interaction between the "free spins" at the chain edges. Edge effects can, therefore, not explain the ferromagnetic Weiss term in $\chi_{\|}(T)$. We, therefore, believe that the upturn in $\chi_{\|}(T)$ is intrinsic to $Yb_4As_3$ and is caused by a weak ferromagnetic interchain coupling.

To investigate the susceptibility of $Yb_4As_3$ at sufficiently low temperatures, where the interchain-coupling effects become important, we measured the ac-susceptibility $\chi_{ac}$ (Figure 4). The absolute values of $\chi_{ac}$ have been determined by calibrating them at the dc-susceptibility measured in the temperature range $2\,\mathrm{K} \leq T \leq 6\,\mathrm{K}$ using a SQUID magnetometer at 50 mT.[43,44] For $T \geq 0.4\,\mathrm{K}$, $\chi_{ac}(T)$ agrees well with the theoretical curve using the same parameters as given by Oshikawa *et al.*[30] At a temperature $T = 0.12\,\mathrm{K}$, a cusp-like anomaly occurs which broadens substantially and shifts to lower temperatures upon superimposing small dc fields $B_a \leq 0.01\,\mathrm{T}$, characteristic for spin-glass freezing. This temperature is of the same order of magnitude but somewhat higher than $T = 0.045\,\mathrm{K}$, which is the upper boundary for magnetic ordering with moments larger than $0.15\,\mu_B$ as inferred from $^{170}Yb$ Mössbauer spectroscopy.[5]

We have performed the $\chi_{ac}(T, \nu)$ measurements at various frequencies $\nu$ of the applied ac-field. The relative shift $\delta = \Delta T_f/(\Delta \log(2\pi\nu) \cdot T_f)$ of the freezing temperature $T_f$ per decade in the frequency $\nu$ is estimated to be $\delta = 0.03 \pm 0.005$. This value is just between typical values for the shift in metallic spin glasses, e. g., CuMn: $\delta = 0.005$, and insulating ones, e.g. (EuSr)S: $\delta = 0.06$.[42]

To investigate whether domain disorder affects the spin-glass behavior, we studied the anisotropy of $\chi_{ac}(T)$. Our preliminary result is that the low-$T$ susceptibility for a monodomain $Yb_4As_3$ crystal measured parallel to the $Yb^{3+}$-chains $\chi_{\|}(0.1\,\mathrm{K})$ equals that of about $0.6 \cdot \chi_m(0.1\,\mathrm{K})$, where $\chi_m(0.1\,\mathrm{K})$ is the value found for a polydomain $Yb_4As_3$ crystal. The spin-glass cusp is also present in $\chi_{\|}(T)$, and the freezing temperature is not changed. This provides evidence that disorder on a smaller scale than the domain disorder is the cause for the spin-glass effects in $Yb_4As_3$.

On the other hand, a broad peak in the low-$T$ specific heat measured on a polydomain sample around 0.17 K was attributed to spin-glass-type effects as well:[21,41] (a) The upturn in $C(T)/T$ measured at fixed field can be well described by a $1/T^3$ dependence. This describes the high-$T$ tail of a nuclear Schottky anomaly involving an average "internal field" $B_{av} \approx 56\,\mathrm{T}$ which is forming in the spin-glass state and is acting on the nuclear spins of the $^{171}Yb$, $^{173}Yb$, and $^{75}As$ isotopes.[21] The average magnetic moment of the $Yb^{3+}$-ions amounts to $\bar{\mu} \approx 0.5\mu_B$. (b) The field dependence of the peak at $T = 0.17\,\mathrm{K}$ which is obtained after subtracting the "upturn" from the raw data is typical for spin glasses.[21,41,42]

In addition, we measured the specific heat on a monodomain sample of $Yb_4As_3$ in magnetic fields up to 4 T applied parallel to the trigonal axis in the temperature range $0.08\,\mathrm{K} \leq T \leq 1\,\mathrm{K}$.[45] The anisotropy of the low-temperature susceptibility of the sample showed that at least 98 % of the sample volume formed a single domain. As is the case for the polydomain sample, the zero-field data show the low-temperature upturn which apparently masks the shoulder-like anomaly due to the spin-glass freezing. By increasing the applied magnetic field, one can resolve this anomaly. Furthermore one observes that it broadens substantially and is shifted towards higher temperatures. These observations again clearly indicate that disorder on a scale smaller than the domain size causes the spin-glass freezing. In contrast to the measurement on the polydomain sample, the suppression of $C(T, B)/T$ at low $T$ as a function of the applied field is distinctly smaller upon applying fields with $B \geq 1\,\mathrm{T}$.

In summary, the *antiferromagnetic* intrachain coupling together with the *ferromagnetic* interchain coupling leads to strong frustration in the hexagonal arrangement of the spin chains. Together with the disorder that is present on the $Yb^{3+}$-chains, as inferred, e. g., from the relative short charge-carrier mean free path $\ell \approx 215\,\text{Å}$ obtained from Shubnikov-de Haas experiments,[44] the observed spin-glass effects can be understood quite naturally. Furthermore, due to the finite homogeneity range of $Yb_4As_3$, Yb (and also As) vacancies at concentrations of up to several percent per formula unit are expected in single-phase samples.[46]

## §5. Summary

We have presented an overview over the experimental and theoretical results on the charge-ordering transition and the low-temperature onedimensional magnetism of $Yb_4As_3$, together with recent results on the low-temperature ac-susceptibility, the specific heat in large magnetic fields, and the specific heat of a monodomain sample in varying magnetic fields. The charge-ordering in this compound and its P- and Sb-doped mixed crystals, driven by the strong intersite Coulomb forces between the $Yb^{3+}$-ions, is the central key for the understanding of its low-temperature properties. Due to the charge ordering, the electronic structure of the crystal develops at $B = 0$ to that of a quasi-onedimensional Heisenberg antiferromagnet as the temperature is lowered to $T \ll T_{co}$: The large heavy-fermion like specific-heat $\gamma$ value, the absolute value and temperature dependence of the magnetic susceptibility, and the occurrence of spin excitations whose spectra can be accurately described by the des Cloizeaux-Pearson two-spinon continuum are only some of the experimental results giving a proof for the formation of the antiferromagnetic $S = 1/2$ spin chains in the system.

We have observed a drastic dependence of the thermodynamic quantities on transverse magnetic fields, in particular at temperatures below about 2 K. These can be understood within the framework of an effective Heisenberg Hamiltonian with an additional antisymmetric alternating exchange interaction, leading to an internal staggered magnetic field. Our analysis of the low-temperature upturn in the magnetic susceptibility and the occurrence of spin-glass freezing at very low temperatures $T \leq 0.12$ K give evidence for a weak ferromagnetic interchain coupling. The comparatively small suppression of the specific-heat $\gamma$ value using a monodomain sample in a field applied parallel to the spin chains gives further support for this scenario.


1) P. Fulde: Ann. Phys. **6** (1997) 178.
2) E. J. W. Verwey and P. W. Haaymann: Physica **8** (1941) 979.
3) A. Yaresko, V. Antonov, H. Eschrig, P. Thalmeier and P. Fulde: Phys. Rev. B **62** (2000) 15538.
4) M. O'Keeffe and S. Andersson: Acta Cryst. A **33** (1977) 914.
5) P. Bonville, A. Ochiai, T. Suzuki and E. Vincent: J. Phys. I France **4** (1994) 595.
6) A. Ochiai, T. Suzuki and T. Kasuya: J. Phys. Soc. Jpn. **59** (1990) 4129.
7) K. Iwasa, M. Kohgi, N. Nakajima, R. Yoshitake, Y. Hisazaki, H. Osumi, K. Tajima, N. Wakabayashi, Y. Haga, A. Ochiai, T. Suzuki and A. Uesawa: J. Magn. Magn. Mat. **177–181** (1998) 393.
8) P. Fulde, B. Schmidt and P. Thalmeier: Europhys. Lett. **31** (1995) 323.
9) K. Takegahara and Y. Kaneta: J. Phys. Soc. Jpn. **60** (1991) 4009.
10) J. Labbé and J. Friedel: J. Phys. France **27** (1966) 153.
11) M. Rams, K. Królas, K. Tomala, A. Ochiai and T. Suzuki: Hyperfine Interactions **97–98** (1996) 125.
12) M. Kohgi, K. Isawa, A. Ochiai, T. Suzuki, J.-M. Mignot, B. Gillon, A. Gukasov, J. Schweizer, K. Kakurai, M. Nishi, A. Dönni and T. Osakabe: Physica B **230–232** (1997) 638.
13) K. Iwasa, M. Kohgi, A. Gukasov, J.-M. Mignot, A. Ochiai, H. Aoki and T. Suzuki: Physica B **281 & 282** (2000) 460.
14) S. Suga, A. Ochiai, T. Suzuki, H. Harada, A. Sekiyama, T. Matsushita, T. Iwasaki, A. Kimura, M. Tsunekawa, T. Muro, S. Ueda, H. Daimon, S. Imada, H. Namatame, M. Taniguchi, H. Ishii, T. Miyahara, T. Hanyu and A. Fujimori: J. Phys. Soc. Jpn. **67** (1998) 3552.
15) U. Staub, B. D. Patterson, C. Schulze-Briese, F. Fauth, M. Shi, L. Soderholm, G. B. M. Vaughan and A. Ochiai: Europhys. Lett. **53** (2001) 72.
16) H. G. von Schnering: private communication.
17) V. N. Antonov, A. N. Yaresko, A. Ya. Perlov, P. Thalmeier, P. Fulde, P. M. Oppeneer and H. Eschrig: Phys. Rev. B **58** (1998) 9752.
18) O. Nakamura, N. Tomonaga, A. Ochiai and T. Suzuki: Physica B **171** (1991) 377.
19) A. Ochiai, H. Aoki, T. Suzuki, R. Helfrich and F. Steglich: Physica B **230–232** (1997) 708.
20) H. Aoki, A. Ochiai, T. Suzuki, R. Helfrich and F. Steglich: Physica B **230–232** (1997) 698.
21) R. Helfrich: Ph. D. thesis, Darmstadt (1996), unpublished.
22) M. Kohgi, K. Isawa, J.-M. Mignot, N. Pyka, A. Ochiai, H. Aoki and T. Suzuki: Physica B **259–261** (1999) 269.
23) J. des Cloizeaux and J. J. Pearson: Phys. Rev. **128** (1962) 2131.
24) G. Müller, H. Beck and I. C. Bonner: Phys. Rev. Lett. **43** (1979) 75.
25) A. H. Bougourzi, M. Couture and M. Kacir: Phys. Rev. B **54** (1996) 12 669.
26) M. Köppen, M. Lang, R. Helfrich, F. Steglich, P. Thalmeier, B. Schmidt, B. Wand, D. Pankert, H. Benner, H. Aoki and A. Ochiai: Phys. Rev. Lett. **82** (1999) 4548.
27) F. Steglich, M. Köppen, P. Gegenwart, T. Cichorek, B. Wand, M. Lang, P. Thalmeier and B. Schmidt: Acta Phys. Pol. A **97** (2000) 91.
28) B. Schmidt, P. Thalmeier and P. Fulde: Europhys. Lett. **35** (1996) 109.
29) G. Uimin, Y. Kudasov, P. Fulde and A. Ovchinnikov: Eur. Phys. J. B **16** (2000) 241.
30) M. Oshikawa, K. Ueda, H. Aoki, A. Ochiai and M. Kohgi: J. Phys. Soc. Jpn. **68** (1999) 3181.
31) H. Shiba, K. Ueda and O. Sakai: J. Phys. Soc. Jpn. **69** (2000) 1493.
32) D. C. Dender, P. R. Hammar, D. N. Reich, C. Broholm and G. Aeppli: Phys. Rev. Lett. **79** (1997) 1750.
33) M. Oshikawa and I. Affleck: Phys. Rev. Lett. **79** (1997) 2883.
34) M. Kohgi, K. Iwasa, J.-M. Mignot, B. Fåk, P. Gegenwart, M. Lang, A. Ochiai and H. Aoki: Phys. Rev. Lett. **86** (2001) 2439.
35) K. Iwasa, M. Kohgi, A. Gukasov, J.-M. Mignot, N. Shibata, A. Ochiai, H. Aoki and T. Suzuki: J. Magn. Magn. Mat. **226–230** (2001) 441.
36) N. Shibata and K. Ueda: preprint, cond-mat/0107561.
37) H. Aoki: Ph. D. thesis, Tohoku Univ. (2000), unpublished.
38) H. Aoki, A. Ochiai, M. Oshikawa and K. Ueda: Physica B **281 & 282** (2000) 465.
39) S. Eggert, I. Affleck and M. Takahashi: Phys. Rev. Lett. **73** (1994) 332.
40) M. Kohgi, K. Iwasa, J.-M. Mignot, A. Ochiai and T. Suzuki: Phys. Rev. B **56** (1997) R 11388.
41) R. Helfrich, M. Köppen, M. Lang, F. Steglich and A. Ochiai: J. Magn. Magn. Mat. **177–181** (1998) 309.
42) J. A. Mydosh: *Spin glasses: an experimental introduction.* Taylor & Francis; London, Washington D. C. 1993.
43) P. Gegenwart, T. Cichorek, J. Custers, M. Lang, H. Aoki, A. Ochiai and F. Steglich: J. Magn. Magn. Mat. **226–230** (2001) 630.
44) P. Gegenwart, H. Aoki, T. Cichorek, J. Custers, N. Harrison, M. Jaime, M. Lang, A. Ochiai and F. Steglich: Physica B (2002), in press.
45) H. Aoki, T. Cichorek, P. Gegenwart, J. Custers, M. Lang, A. Ochiai and F. Steglich: Physica B (2002), in press.
46) U. Burkhardt, Y. Grin and H. G. von Schnering: Abstract PA 124, *VI*$^{th}$ *European Conference on Solid State Chemistry* (Zürich 1997).